OBJECT IDENTIFICATION USING MULTIFREQUENCY EMI DATA

Dr. Dean Keiswetter and Dr. I.J. Won
Geophex, Ltd.
605 Mercury Street
Raleigh, NC 27603
Phone: (919) 839-8515
Fax (919) 839-8528
E-mail: keiswetter@geophex.com / ijwon@geophex.com

Dr. Bruce Barrow and Dr. Tom Bell
AETC Incorporated
1225 Jefferson Davis Highway
Arlington, Virginia, 22202
Phone: (703) 413-0500
Fax (703) 413-0512
E-mail: bjb@va.aetc.com / tbell@va.aetc.com

Detection Technology Session

Abstract

Unexploded ordnance (UXO) cleanup is a top priority Army Cleanup Problem requirement and is identified as a major problem throughout the Department of Defense. A recent SERDP technical report summarizes the status of capability for buried UXO detection, discrimination, and identification as follows: (a) can detect UXO, within definable limits; (b) cannot effectively discriminate UXO anomalies from 'false alarm' anomalies; and (c) cannot identify UXO. False alarm anomalies are defined here as geophysical anomalies caused by buried UXO debris, other metallic objects, gravel and cobbles, soil heterogeneities, tree roots, and other natural and cultural features. False alarm anomalies significantly contribute to the cost of UXO remediation due to the large number of unnecessary excavations. A major initiative in the research and development community, therefore, is to develop discrimination (target identification) capabilities. One potential methodology for target identification involves utilizing the broadband scattered electromagnetic induction response. This technique, which is known as Electromagnetic Induction Spectroscopy (EMIS), has recently become feasible due to the development of the GEM-3 sensor. The GEM-3 is an efficient, broadband, handheld EMI sensor than employs a unique monostatic coil design. Analyzing the EMI spectral content for target identification is not new. In fact, elementary EM theory states that an object must exhibit different responses at different frequencies. All fundamental EM equations involving a time-varying source testify as such. By fully characterizing and identifying an object without excavation, we should be able to significantly reduce the number of false targets. EMIS should be fully applicable to many other problems where target identification and recognition (without intrusive search) are important.

Introduction

Geophysical sensors for detecting UXO are typically limited to magnetometers and EMI-based metal detectors. A magnetometer can detect only ferrous objects. Metal detectors can detect both ferrous and nonferrous targets; thus, they are more useful as stand-alone sensors than magnetometers. Despite popular interest and enthusiasm, ground-probing radar (GPR) has yet to demonstrate its usefulness as a stand-alone sensor.

Conventional metal detectors are not designed to do any more than simply detect the presence of buried metal objects, because most of them operate at a factory-set single frequency. A few detectors may have capability of operating at two or so discrete frequencies. These detectors have no ability to discriminate ordnance from trash metals and, therefore, the false alarm rate is unacceptably high. We believe that the EMIS technology can provide both detection and discrimination capabilities.

Our main interest in this article is the frequency dependence of the EMI response. By measuring an object's EMI response in a broad frequency band, we attempt to detect and characterize the object's geometry and material composition. This new technology exploiting the spectral EMI response is known as the Electromagnetic Induction Spectroscopy (EMIS)

When an electrically conductive and/or magnetically permeable object is placed in a time-varying electromagnetic field, a system of induced current flows through the object. By observing a small secondary magnetic field emanating from the induced current, we attempt to detect the object; this is the foundation of the time-honored electromagnetic induction (EMI) method. EMI physics is completely described by Maxwell's four equations, although analytical solutions beyond the simplest geometry are rare due to mathematical complexity.

Elementary EM theory states that an object must exhibit different responses at different frequencies. All fundamental EM equations involving a time-varying source testify as such. The reason why the subject has not been explored, in our opinion, is due to the lack of practical broadband EMI instruments to study the phenomenon. On the research level, however, there have been many experimental works that studied broadband EMI phenomena [1-4].

GEM-3: A Multifrequency EMI sensor

The GEM-3 (Figure 1) uses a pair of concentric, circular coils to transmit a continuous, broadband, digital, EM waveform [5, 6]. The resulting field induces a current in the earth as well as in any nearby conductive materials. The set of two transmitter coils, with precisely computed dimensions and placement, creates a zone of magnetic cavity (i.e., an area with a vanishing primary magnetic flux) at the center of the two coils. A third receiving coil is placed within this magnetic cavity so that it senses only the weak, secondary field returned from the earth and buried targets. All coils are molded into a single, light, circular disk in a fixed geometry, rendering a very portable, monostatic sensor head. The removable electronics package controls system operations and stores the digital data.

For a frequency-domain operation, the GEM-3 prompts for a set of desired transmitter frequencies. Built-in software converts these frequencies into a digital "bit-stream," which is used to construct

the desired transmitter waveform for a particular survey. The bit-stream controls a set of digital switches (called H-bridge) connected across the transmitter coil, and generates a complex waveform that contains all frequencies specified by the operator. This method of constructing an arbitrary waveform from a digital bit-stream is known as the pulse-width modulation technique.

The monostatic configuration has many advantages; including, a compact sensor head, large transmitter moment, high spatial resolution, no spatial distortion (common to bistatic sensors), and circular symmetry that greatly simplifies the mathematical analysis and modeling processes. The digital design of the GEM-3 allows it to transmit any digitized waveform. It can, therefore, transmit pulses, random binary sequences, or composite frequency waveforms, and record either frequency- or time-domain data.

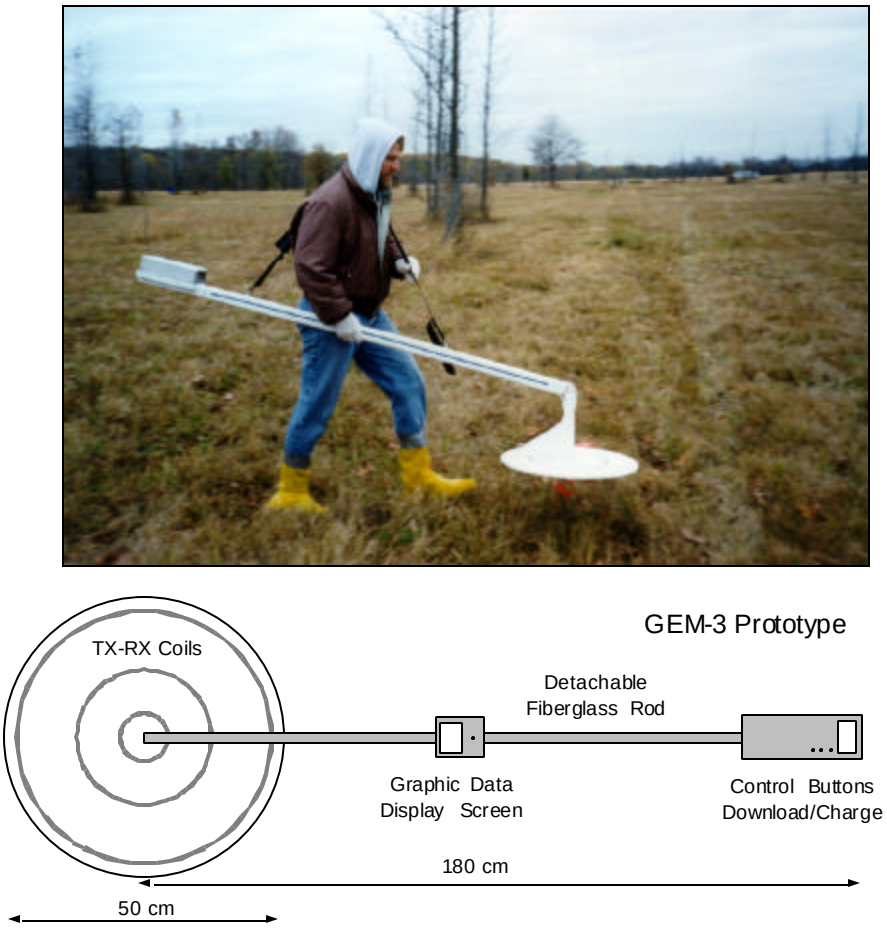

Figure 1.GEM-3 sensor in operation.

The theoretical basis for EMIS has been developed in previous articles [7-12]. In this article, we present synthetic and empirical evidence regarding the application of EMIS for discrimination of UXO.

Multifrequency EMI Data

In this section, we present GEM-3 data acquired during Jefferson Proving Ground Phase IV Demonstration and present the analysis procedures. Our approach to the JPG Phase IV Demonstration addresses the feasibility of correlating the broadband signature of an unknown buried object to a library of EMI spectral signatures for known targets. The objective, therefore, focuses on identifying targets (the essence of the false alarm problem) based on their EMI spectral response.

Experimental Setup and Analysis of Multifrequency EMI Data

Prior to the field demonstration, we measured the EMI response of various UXO and non-UXO items using the GEM-3 sensor. For these measurements, the sensor was held rigidly in place on a wooden platform over one meter above the ground. The objects were individually placed directly under the sensor head. The distance (sensor to target) and orientation (relative to the primary field) varied over a wide range.

Data collection was controlled by a laptop PC. Multiple broadband sweeps were collected and downloaded to and ASCII file on the PC in real-time. The frequency range of the data collected was from 30 Hz to 23,970 Hz. We recorded multifrequency EM data for numerous UXO targets (including, a variety of projectiles and mortars) and non-UXO targets (flat disks, I-beam, pipes, and plates). These signatures were used as the reference library.

Multifrequency EMI data were then acquired over the 160 buried targets (note that the targets were included in the library). Because the measured spectral response is sensitive to a number of sensor/target parameters (viz., location, depth, and orientation), we recorded multifrequency EM data on a three feet by three feet grid centered over the target.

Two levels of analysis were applied to the spatial grid of GEM-3 spectral data. The first method was a straightforward comparison of the measured data at discrete locations in the grid to the library of measurements collected with ordnance and clutter items above ground. The second method was to use a simple model to invert the data at all locations to solve for the model parameters of: location, depth, orientation, and normalized GEM-3 response spectra along and across the ordnance's symmetry axis [13]. The normalized response spectra were again compared to the data collected with the items above ground.

With the first method, a spatial cut of data through a given point was plotted of the inphase GEM-3 response versus the quadrature response for all frequencies. Figure 2 shows an example of this "I-Q" type of plot. An interactive interface was developed that would compare the discrete I-Q ratios of the data to the library of measurements made above ground with the ordnance at fixed distances and several orientations. An arbitrary scaling factor was allowed in the comparison to correct for a different depth of the object relative to the library. A linear combination of the horizontal and vertical signatures of a given library item was allowed to correct for object orientations not in the library. Each library item was then ranked in order of RMS difference from the measurement with the minimum RMS difference being the most likely library match. In Figure 2, the triangles correspond to the I-Q data of the measurement and the

asterisks correspond to the closest library match. In this case, the library measurement of the 20mm ordnance item tilted 45 degrees and scaled 0.35 provides the closest match.

There are several limitations with this library matching technique. The primary one is the sensitivity of the GEM-3 data to a variety of ordnance/clutter parameters: location, depth, and orientation. It was not feasible to collect all of the necessary library signatures for the variety of ordnance and clutter items. A subset of measurements directly over the object at one or two expected depths and five orientations (horizontal, nose-up, nose-down, 45 degrees nose-up, and 45-degrees nose-down) was settled on as a minimal signature library. The second problem is that it does not take advantage of the spatial variation in the signature as the GEM-3 moves over the object. The signature library obtained was only good directly above the object. Lastly, there is some overlap in library signatures between the ordnance and clutter items. A given projectile at a certain depth and orientation may resemble a clutter object at another depth and orientation. In an effort to address these shortcomings, a simple empirical model was developed.

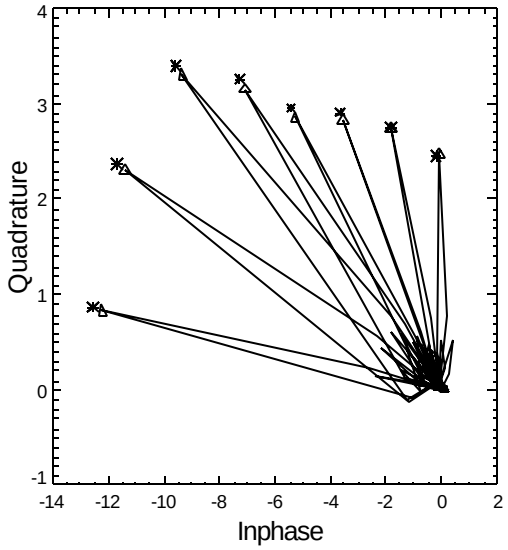

Figure 2. Plot of inphase versus quadrature response of GEM-3 at eight frequencies over an unknown object at 25 spatial locations. The triangles plot the maximum measured response at the x,y location of (0,0). The asterisks are from the signature library (known target). In this case, the unknown target correlates with a 20-mm projectile, tilted 45 degrees from vertical.

To first order, the response of a compact object to the GEM-3's time varying field can be modeled as an induced dipole response. The strength of this dipole field is determined by the physical characteristics of the object (the electrical properties of the metal and the shape of the object) and the strength of the GEM-3's transmitted field along the physical axes of the object. For symmetrical objects like ordnance, it is the strength of the field along the length of the ordnance and the strength of the field perpendicular to this that is important. Empirically, one can express the induced dipole moment, m, as $m_l = ß_l H_l$ and $m_t = ß_t H_t$ where l denotes along and t denotes transverse to the ordnance's primary axis, the $ß$'s are the normalized responses characteristic of each object, and H is the field from the GEM. For each object, there are four

ßs: inphase and quadrature, along and transverse. These ßs are a function of frequency and have, for each object, been determined from the in air measurements. Figure 3 plots these parameters as a function of frequency for (a) the 20mm, (b) a small metal pipe and (c) a small metal disk. If these characteristic ß spectra differ significantly, then one can discriminate between the objects. In this example, the disk is quite different from the 20mm, but the pipe is not.

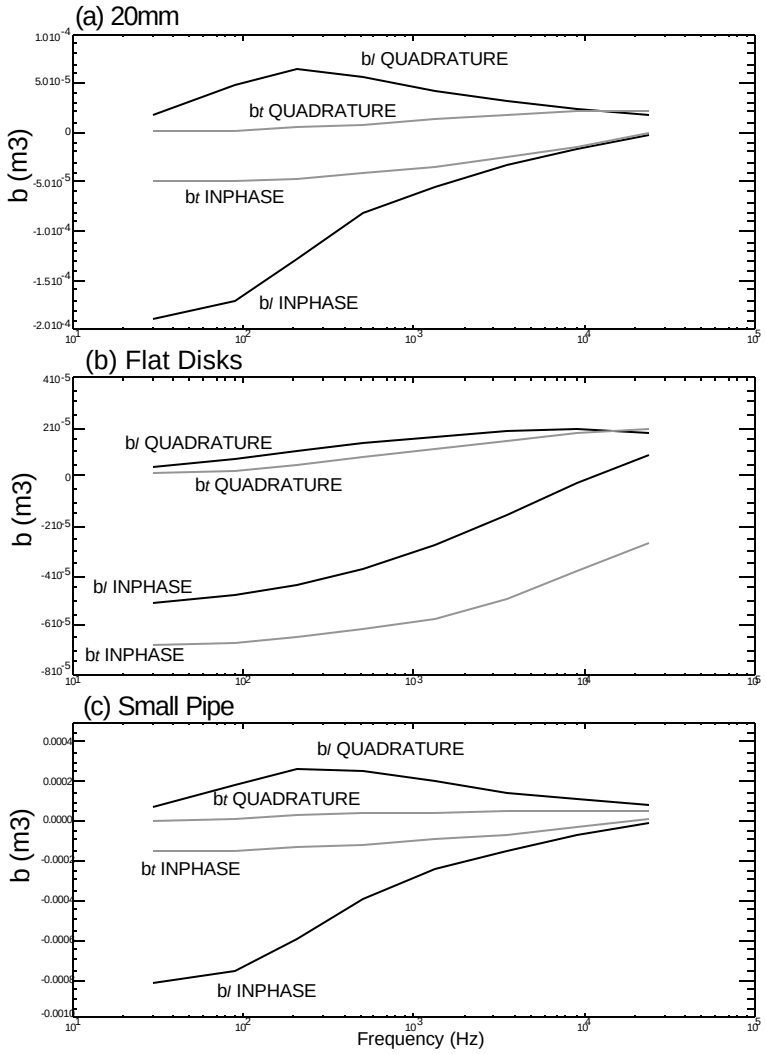

Figure 3. Beta (ß) response spectra along (l) and transverse (t) to an object's symmetry axis calculated from in-air measurements made by the Gem-3 for a 20-mm (a), flat disk (b), and small pipe (c).

The induced dipole moment determines the response strength of the GEM-3. Because of this, given a sufficient set of spatial measurements over an unknown object, the model parameters of location, depth, orientation, and ß spectra can be determined. Figure 4 shows the contours of GEM-3 inphase response spatially over an unknown object. A contour is shown for each of the eight frequencies collected. The dashed lines represent the best model fit to this data. The best-fit parameters for this object placed it at a depth of 0.05m, an azimuth angle of 135 degrees and a

declination angle of 45 degrees. Figure 5 plots the best fit spectra and the dashed line represents the spectra of a 20mm from the library signatures.

Although the results appear very promising, several challenges remain. (1) For the range of frequencies collected, some of the ordnance and clutter items had very similar spectra. As expected, non-UXO targets that closely resemble UXO produce similar EMI signatures. (2) Higher order effects were also found to be a problem. This effect was primarily observed for targets that are very shallow or those that have complicating factors such as aluminum fins. (3) The model assumes a uniform field. Due to the size of some targets (especially when buried vertical),the transmit field is not uniform across the larger objects. For these objects, the dipole model was a less accurate description of the data collected. In future work, we hope to address this issue. Lastly, a significant background effect was observed over some unknown objects. Characteristically, this effect was observed as a spatially varying signal over the object that was constant as a function of frequency in the inphase but negligible in the quadrature. It is not clear if this was caused by the uneven ground surface over some of the objects or by some characteristic of the disturbed soil.

Conclusions

The broadband EMI response of an individual item is a function of its composition, size, shape, orientation, and burial depth. To isolate effects associated with orientation of the object, we must interrogate that target with multiple orientations of the primary field. To fully realize its potential as a new technology, however, we need to further develop broadband EMI models and advance the sensor hardware and software.

The EMIS method, when completed, should be particularly useful for detecting and identifying unexploded ordnance. By fully characterizing and identifying an object without excavation, we will be able to significantly reduce the number of false alarms. Target identification using EMIS principles is directly applicable to other problems where the target identification and recognition (without intrusive search) are important.

Acknowledgements

This study was funded by the Naval Surface Warfare Center – Jefferson Proving Ground Phase IV Program. The GEM-3 sensor is the product of many Geophex scientists and engineers including, Joe Seibert, David Chen, and Alex Gladkov.

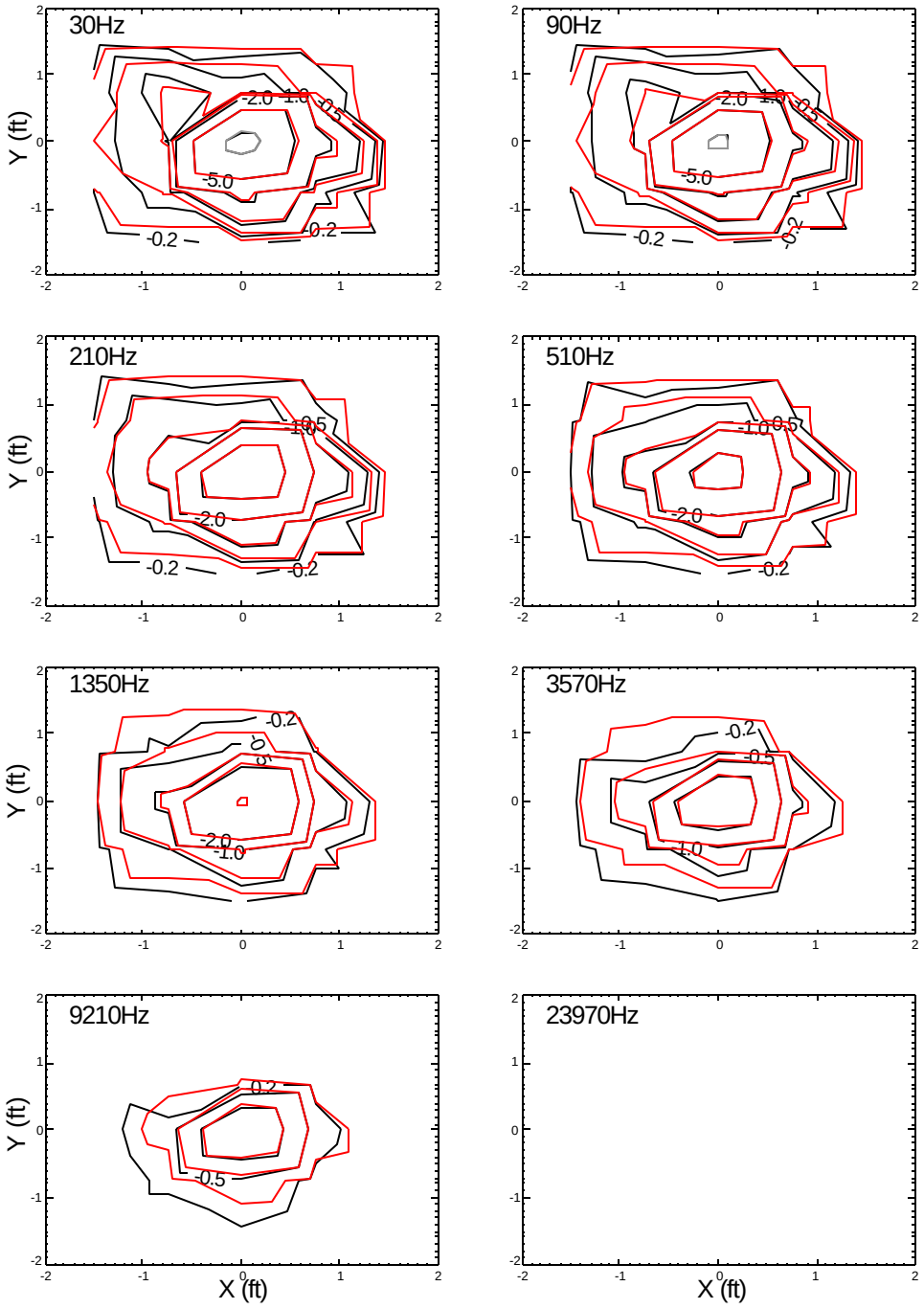

Figure 4. Contours of spatial GEM-3 response at eight frequencies. Red contours represent best model fit using the parameter estimating procedure. In this case the best fit is a 20-mm projectile at x=-0.05m, y=0.0m, z=0.15m, azimuth of 135 degrees, and declination of 45 degrees.

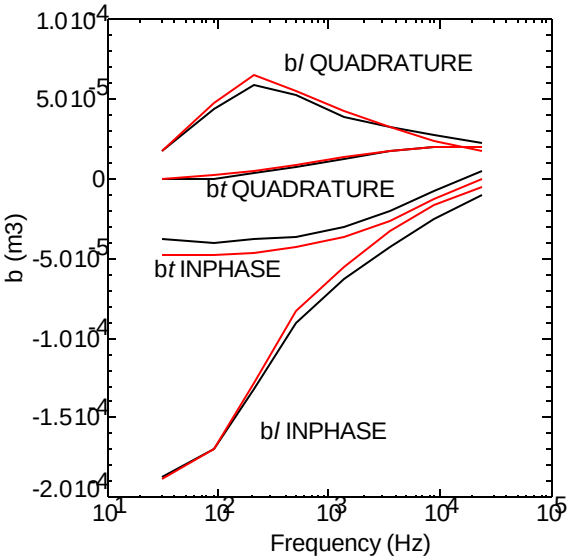

Figure 5. Comparison of best-fit β spectra for the unknown object (red) to spectra measured for the 20-mm projectile (black).

References

1. Ryu, J., Morrison, H.F., and Ward, S.H., 1972, Electromagnetic depth sounding experiment across Santa Clara Valley, *Geophysics*, v. 37, p. 351-374.
2. Ward, S. H., Pridmore, D. F., Rijo, L., and Glenn, W. E., 1974, Multispectral electromagnetic exploration for sulfides, *Geophysics*, v. 39, p. 662-682.
3. Won, I. J., 1980, A wide-band electromagnetic exploration method: some theoretical and experimental results, *Geophysics*, v. 45, p. 928-940.
4. Won, I. J., 1983, A sweep frequency electromagnetic method, Chapter 2 in *Development of Geophysical Exploration Method - 4*, Editor A.A. Fitch, Elsevier Applied Science Publishers, Ltd., London, p. 39-64.
5. Won, I. J., Keiswetter, D. A., Fields, G. R. A., and Sutton, L. C., 1996, GEM-2: a new multifrequency electromagnetic sensor, *Jour. Environmental and Engineering Geophysics*, Vol. 1, No. 2, p. 129-138.
6. Won, I. J., Keiswetter, D. A., Hanson, D. R., Novikova, E., and Hall, T. M., 1997, GEM-3: a monostatic broadband electromagnetic induction sensor, *Jour. Environmental and Engineering Geophysics*, Vol. 2, Issue 1, p. 53-64.
7. Wait, J. R., 1951, A conducting sphere in a time-varying magnetic field, *Geophysics*, v. 16, p. 666-672.
8. Wait, J. R., 1953, A conducting permeable sphere in the presence of a coil carrying an oscillating current, *Canadian Jour. Physics*, v. 31, p. 670-678.
9. Wait, J. R., 1959, Some solutions for electromagnetic problems involving spheroidal, spherical, and cylindrical bodies, *J. Res. N.B.S.* (Mathematics and Mathematical Physics), v. 64B, p. 15-32.
10. Wait, J. R., 1960, On the electromagnetic response of a conducting sphere to a dipole field, *Geophysics*, v. 25, p. 619-658.
11. Wait, J. R., 1969, Electromagnetic induction in a solid conducting sphere enclosed by a thin conducting spherical shell, *Geophysics*, v. 34, p. 753-759.
12. Fuller, B. D., 1971, Electromagnetic response of a conductive sphere surrounded by a conductive shell, *Geophysics*, v. 36, p. 9-24.
13. Barrow, B., DiMarco, R., Khadr, N., and Nelson, H., 1997, Processing and analysis of UXO signatures measured with MTADS, Proc. UXO Forum, p. 8-18.